JOURNAL OF VIROLOGY, Aug. 2006, p. 7405–7415 Vol. 80, No. 15
0022-538X/06/$08.00+0 doi:10.1128/JVI.02533-05

Intramolecular and Intermolecular Uridylylation by Poliovirus RNA-Dependent RNA Polymerase

Oliver C. Richards,[1] Jeannie F. Spagnolo,[2] John M. Lyle,[2]† Susan E. Vleck,[2] Robert D. Kuchta,[1] and Karla Kirkegaard[2]*

Department of Chemistry and Biochemistry, University of Colorado, Boulder, Colorado,[1] and Department of Microbiology and Immunology, Stanford University School of Medicine, Stanford, California[2]

Received 4 December 2005/Accepted 4 May 2006

The 22-amino-acid protein VPg can be uridylylated in solution by purified poliovirus 3D polymerase in a template-dependent reaction thought to mimic primer formation during RNA amplification in infected cells. In the cell, the template used for the reaction is a hairpin RNA termed 2C-*cre* and, possibly, the poly(A) at the 3′ end of the viral genome. Here, we identify several additional substrates for uridylylation by poliovirus 3D polymerase. In the presence of a 15-nucleotide (nt) RNA template, the poliovirus polymerase uridylylates other polymerase molecules in an intermolecular reaction that occurs in a single step, as judged by the chirality of the resulting phosphodiester linkage. Phosphate chirality experiments also showed that VPg uridylylation can occur by a single step; therefore, there is no obligatory uridylylated intermediate in the formation of uridylylated VPg. Other poliovirus proteins that could be uridylylated by 3D polymerase in solution were viral 3CD and 3AB proteins. Strong effects of both RNA and protein ligands on the efficiency and the specificity of the uridylylation reaction were observed: uridylylation of 3D polymerase and 3CD protein was stimulated by the addition of viral protein 3AB, and, when the template was poly(A) instead of the 15-nt RNA, the uridylylation of 3D polymerase itself became intramolecular instead of intermolecular. Finally, an antiuridine antibody identified uridylylated viral 3D polymerase and 3CD protein, as well as a 65- to 70-kDa host protein, in lysates of virus-infected human cells.

Many positive-sense single-stranded RNA viral genomes are relatively small templates that encode information for complex viral replication cycles and thus require highly efficient utilization of limited coding capacity. The number of functional activities expressed from any genome can be expanded by utilizing both precursor polypeptides and their processed cleavage products. For example, poliovirus protein 3D is an RNA-dependent RNA polymerase, while its presumed precursor, 3CD, which is a fusion between the 3C protease and 3D polymerase, manifests no polymerase activity but functions as a specific protease with substrate recognition properties different from its cleavage product, 3C protease (29, 68). Another mechanism that expands coding capacity is the utilization of the same polypeptide for multiple functions. For example, in addition to proteolytic activity, 3CD also functions as a specific RNA-binding protein with crucial roles in viral RNA replication. It binds the 5′-terminal RNA cloverleaf structure (2, 3, 23, 49) as well as an internal stem-loop structure in the 2C coding region (66, 67); both interactions are required for the initiation of RNA replication. Finally, posttranslational modifications can further modify the function of viral proteins; for example, the covalent myristoylation of viral capsid protein VP0 facilitates its transition from a precursor protein to a component of an assembled capsid (4, 42).

The poliovirus genome contains a single open reading frame that codes for a polyprotein of 247,000 Da that is cleaved by viral proteases to produce both structural and nonstructural viral proteins. 3D polymerase is located at the C-terminal end of the polyprotein. It is the core polypeptide that catalyzes the synthesis of RNA chains from both negative- and positive-strand templates. All classes of nucleic acid polymerases consist of three major subdomains (fingers, palm, and thumb), which adopt the shape of a cupped right hand (40, 60). The active-site cavities of poliovirus polymerase 3D (21, 62) and the polymerases of the closely related rhinoviruses (34) and foot-and-mouth disease virus (14) are formed by residues of the palm subdomain and are encircled by the finger and thumb subdomains.

Unlike some of the larger RNA-dependent RNA polymerases, such as that of hepatitis C virus, that initiate synthesis of cRNA chains directly at the 3′ end of the template strand (54, 69), poliovirus 3D polymerase initiates RNA strand synthesis by elongating a uridylylated protein primer (50), termed VPg or 3B, which consequently constitutes the 5′ terminus of each RNA strand synthesized. Yeast two-hybrid analyses showed that VPg binds directly to 3D polymerase (65). Uridylylation of the VPg primer has been studied in vitro (50). The reaction is catalyzed by 3D polymerase and requires an RNA template to direct the transfer of one or two uridylate residues to VPg. In studies of rhinovirus 14, McKnight and Lemon (38, 39) initially observed an RNA structure within the VP1 coding region that was essential for RNA replication. Subsequently, similar RNA structures, termed "*cis*-acting replication enhancer" or "*cre*" elements, were found in the genomes of other picornaviruses: in the VP2 coding region of Theiler's virus and mengovirus (33), in the 2A coding region of rhinovirus 2 (17),

* Corresponding author. Mailing address: Department of Microbiology and Immunology, Stanford University School of Medicine, 299 Campus Drive, Stanford, CA 94305-5402. Phone: (650) 498-7075. Fax: (650) 498-7147. E-mail: karlak@stanford.edu.

† Present address: Pacific Biosciences, 1505 Adams Drive, Menlo Park, CA 94025.

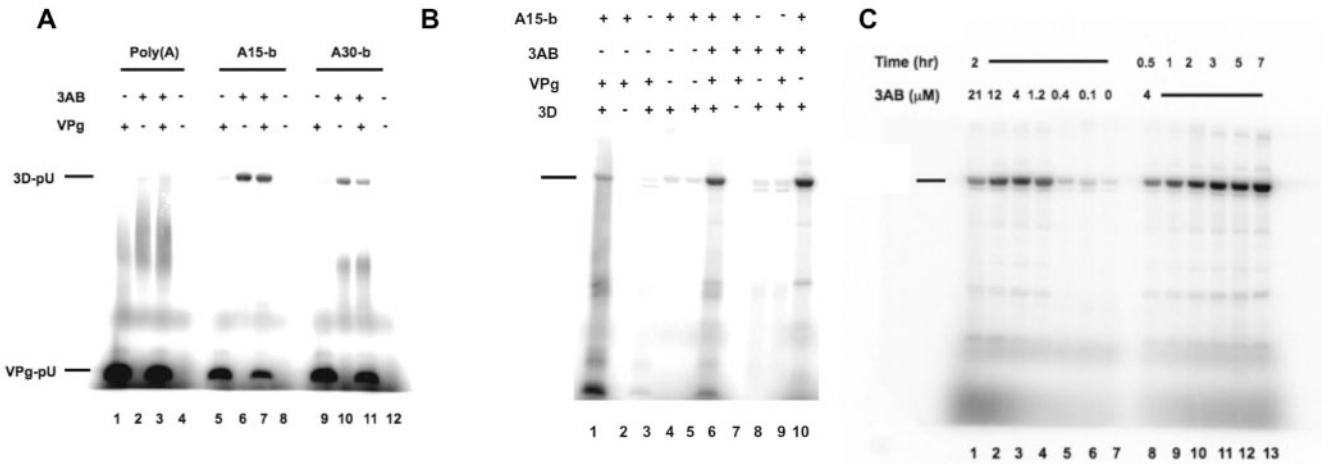

FIG. 1. (A) Template requirements for uridylylation of VPg and 3D polymerase. The incorporation of [^{32}P]UTP into 3D polymerase and VPg, using template poly(A) (lanes 1 to 4), A15-b (lanes 5 to 8), or A30-b (lanes 9 to 12), is illustrated by autoradiography in reactions described in Materials and Methods. Reaction mixtures contained 3D polymerase (2 μM), 3AB (4 μM), and VPg (100 μM) as indicated. Products were digested with RNase A and resolved in 12% polyacrylamide-Tris-Tricine gels. The positions of migration of the 2.5-kDa uridylylated VPg and the 52-kDa uridylylated 3D polymerase are indicated. These assignments were made by the known mobilities of VPg and 3D polymerase in comparison to markers, by the absence of other proteins in the purified preparations, and by immunoblotting (not shown). (B) Basic requirements for uridylylation of 3D polymerase. The incorporation of [^{32}P]UTP into 3D polymerase and VPg is shown, as described in Materials and Methods. Where indicated, A15-b was present at 10 μM, 3AB at 3.6 μM, VPg at 100 μM, [^{32}P]UTP at 0.12 μM (2 μCi/30 μl), and 3D polymerase at 2 μM. Products were resolved in 12% polyacrylamide-Tris-Tricine gels. The positions of uridylylated 3D polymerase and VPg are as in panel A. (C) 3D polymerase uridylylation as a function of 3AB concentration and incubation time. Reaction mixtures (see Materials and Methods) included template A15-b and 3D polymerase (2 μM). Products were digested with RNase A and resolved in 12% polyacrylamide-Tris-Tricine gels, as above. The position of uridylylated 3D polymerase is as in panel A. Unmarked labeled species most likely result from incomplete RNase digestion.

in the 5′-noncoding region of foot-and-mouth-disease virus (37, 44), and in the 2C coding region of poliovirus, 2C-*cre* (18, 51, 55). For poliovirus, not only is the specific stem-loop structure a template for uridylylation of VPg, but this reaction is greatly stimulated by 3CD, which binds to the 2C-*cre* element (63, 64). In vitro, poly(A) can also serve as a template (50). In the cell, it is not yet clear whether 2C-*cre* is used as the template for both positive and negative strands or whether 2C-*cre* is used only for positive-strand synthesis and poly(A) is used for negative-strand synthesis (19, 41, 43).

In this report, we show that 3D polymerase also catalyzes inter- and intramolecular uridylylation of 3D polymerase molecules themselves. The uridylylation of 3D polymerase occurs by a single-step mechanism, as does the uridylylation of VPg, suggesting that these are independent reactions and that one uridylylation step is not an obligate intermediate for the other uridylylation. Not only can 3D polymerase uridylylate itself, but it can also uridylylate 3CD and perhaps even 3AB, as was demonstrated with purified proteins. Two-dimensional gel electrophoresis of extracts from infected cells revealed that both 3D polymerase and the larger, 3D-containing polypeptide 3CD reacted with antiuridine antibodies. Although it is not yet known whether uridylylation of 3D or 3CD alters the function of the protein, such modification may be an additional potential mechanism to increase the spectrum of functions for a genome limited in coding capacity.

MATERIALS AND METHODS

Protein purification. Wild-type Mahoney type 1 poliovirus 3D polymerase and mutant 3D polymerase D328A/D329A were expressed in *Escherichia coli* and purified as described previously (25, 35). An expression plasmid encoding poliovirus 3D polymerase with a C-terminal hemagglutinin (HA) tag (YPYDVPDYA) was engineered by site-directed mutagenesis and verified by sequencing. Unlike several other epitope tags we have tried, 3D-HA was enzymatically active, demonstrating approximately 90% the specific activity of wild-type polymerase in poly(A)-oligo(U) RNA-dependent RNA polymerase assays (data not shown). Poliovirus 3CD containing the mutation C147A in the active site of the 3C protease domain was expressed from a mutagenized pT5T-3CD plasmid and purified in a manner similar to that of 3D polymerase (22). Poliovirus 3AB was expressed from plasmid pT7lac-3AB (provided by A. Paul and E. Wimmer, Stony Brook, NY) in *E. coli* BL21(DE3) and purified according to published procedures (31, 32). Poliovirus VPg (3B) was synthesized by Lofstrand Labs Limited (Gaithersburg, MD) and utilized without further purification.

Enzymes, RNA preparations, and nucleotides. Phosphodiesterase I (snake venom phosphodiesterase) was from U.S. Biochemicals (Piscataway, NJ), and mung bean nuclease was from Promega (Madison, WI). RNase A was purchased from Sigma (St. Louis, MO) and was preheated at 10 mg/ml in 0.1 M sodium acetate, pH 5.0, at 80°C for 10 min before use. A15-b and A30-b are oligonucleotides with continuous stretches of 15 and 30 adenylates, respectively, each with blocked 3′-terminal hydroxyls (inverted deoxyribose) as prepared by Dharmacon Research (Lafayette, CO). Poly(A) was purchased from Amersham-Pharmacia (Piscataway, NJ) with an average size of 300 nucleotides (nt) and was extracted with phenol-chloroform and precipitated with isopropanol. The concentration was based on nucleotide content. The nucleoside triphosphates [α-^{32}P]UTP and [(Sp)α-^{35}S]thio-UTP were obtained from New England Nuclear/Perkin-Elmer (Boston, MA). The labeled thio-UTP contained 99% Sp stereoisomer, according to the manufacturer.

3D uridylylation and analysis of products. Uridylylation of 3D was monitored in 30-μl reaction mixtures that contained 50 mM HEPES (pH 7.2), 3 to 5 μCi [^{32}P]UTP (1.5 μCi in the experiments represented in Fig. 4 and 5), 0.9 μM [(Sp)α-^{35}S]thio-UTP (see Fig. 4 and 5), 5 μM UTP (2 μM in the experiments represented in Fig. 4 and 5), 2 mM dithiothreitol (DTT), 0.5 mM $MnCl_2$, 8% glycerol (10% in the experiments represented in Fig. 2), 10 μM A15-b [1.33 μM poly(A) strands; 6 μM A30-b in the experiments represented in Fig. 1A], 4 to 5 μM 3AB, and 1 to 2 μM 3D polymerase. VPg was added to reactions at 100 μM in the experiments represented in Fig. 1A and 50 μM in the experiments represented in Fig. 5. 3CD was used at 1 μM, where indicated, in the experiments represented in Fig. 6. Reaction mixtures were incubated at 30°C for 2 h except for the experiments represented in Fig. 4 and 5, wherein the [^{32}P]UTP reactions were for 60 min and the [^{35}S]thio-UTP reactions were for 180 min. Variable

reaction times in the experiments represented in Fig. 1B are indicated. NaCl was present at 8 mM in the experiment shown in Fig. 2. Reactions were halted by adjustment to 1 mM EDTA on ice or, in the experiment shown in Fig. 2, by addition of 2 mM EDTA and 100 μg/ml RNase A, followed by 1 h of incubation at 37°C and the addition of sodium dodecyl sulfate (SDS) loading buffer. Samples for the experiments represented in Fig. 4C and 5C were treated with snake venom phosphodiesterase (SVPD), as prescribed by the vendor, at the indicated concentrations at 25°C for 60 min or with mung bean nuclease, as prescribed by the vendor, at 37°C for 30 min. Thereafter, samples were adjusted to 1× sample buffer (5% glycerol, 2.5% β-mercaptoethanol, 1.5% SDS, 0.06 M Tris [pH 6.8], and 0.05% bromphenol blue) and heated at 90°C for 4 min. For the experiments shown in Fig. 1, 4C, and 5C, products were resolved in 12% polyacrylamide-Tris-Tricine gels (10, 58) and gels were transferred to filter paper and dried at 80°C under vacuum. Products in the experiments represented in Fig. 2, 6, and 7 were resolved in 10% polyacrylamide-SDS gels. These gels were stained directly with Sypro Red (see Fig. 2A) (Invitrogen, Carlsbad, CA), dried on filter paper (see Fig. 1, 4C, 5C, and 6) (Whatman, Florham Park, NJ), blotted onto nitrocellulose (see Fig. 7A and 8) (Bio-Rad, Hercules, CA), or blotted onto polyvinylidene difluoride (PVDF) membranes (see Fig. 2B and Fig. 7B and C) (Millipore, Billerica, MA). Radioactive species in dried gels were autoradiographed and quantified by phosphorimager analysis and ImageQuant software (Amersham, Piscataway, NJ). For immunoblot analysis, proteins were transferred to nitrocellulose or PVDF membranes and incubated with polyclonal rabbit antiuridine serum or by polyclonal rabbit anti-3D serum (see Fig. 7 and 8). Antiuridine serum, originally commercially available (Research Plus, Manasquan, NJ), was obtained as the kind gifts of Ann Dvorak (Harvard Medical School, Boston, MA) and David M. Warmflash (University of Houston). The specificity of the antiuridine serum was supported by its lack of reactivity with phosphorylase b, ovalbumin, carbonic anhydrase, trypsin inhibitor, and lactalbumin (data not shown).

Modified procedure for removal of uridylate residues from 3D polymerase. A modified procedure for digestion with SVPD was required to measure removal of UMP moieties from purified 3D polymerase (see Fig. 7A). Purified 3D polymerase at 9 μM was adjusted to 0.1% SDS and denatured by heating at 90°C for 4 min. This preparation was diluted 20-fold to adjust to 0.67 μg polymerase/30 μl, 0.005% SDS, and 1× SVPD buffer (0.1 M Tris-HCl [pH 8.9], 0.1 M NaCl, and 14 mM $MgCl_2$). Stock SVPD (660 U/ml in 50% glycerol, 1× SVPD buffer) was diluted in 1× SVPD buffer to the indicated levels in 2 μl. Digestion proceeded for 60 min at 20°C and was halted by the addition of an equal volume of 2× sample buffer and heating at 90°C for 4 min. Samples were resolved in 10% polyacrylamide-SDS gels, blotted to nitrocellulose, and developed with antiuridine serum (1:3,000), secondary antibody (anti-rabbit, alkaline phosphatase conjugate), and the color development reaction mixture (nitroblue tetrazolium–5-bromo-4-chloro-3-indolylphosphate [NBT-BCIP]; Promega) (7).

Preparation of extracts from poliovirus-infected cells to monitor the time course of appearance of poliovirus proteins. HeLa cells were infected with the Mahoney strain of poliovirus type 1 at a multiplicity of infection (MOI) of 25 PFU/cell. At various times postinfection (0 to 5 h), cells were washed and incubated in 10 mM acetic acid and 18 mM potassium acetate (0°C, 10 min) and suspended in RSB–NP-40 (10 mM Tris [pH 7.5], 10 mM NaCl, 1.5 mM $MgCl_2$, 1% NP-40). Nuclei were removed by centrifugation at 10,000 × *g* (4°C, 10 min), and the supernatants were fractionated in 10% polyacrylamide-SDS gels. Proteins were blotted to PVDF membranes and, in separate blots (see Fig. 7B and C), immunoreactive proteins were reacted with antiuridine (1:2,500) or anti-3D polymerase (1:5,000). After washing of the membranes, proteins were detected with the ECF reagent (Amersham).

Two-dimensional gel analysis of proteins in HeLa extracts. HeLa cells were mock-infected (with phosphate-buffered saline) or infected with wild-type poliovirus or with mutant poliovirus 3D-111 (12) at an MOI of 50 PFU/cell for 5 h at 37°C. The 3D-111 mutant virus displays wild-type growth characteristics but contains two amino acid changes in the 3D polymerase coding region (E98A/D99A). The mutant virus was used because its 3D-containing proteins exhibited a characteristic increased mobility in polyacrylamide-SDS gels compared to their wild-type counterparts that proved useful in the two-dimensional separations. Cells were resuspended in RSB–NP-40 (0°C, 15 min), samples were centrifuged at 10,000 × *g* for 10 min, and the resulting cytoplasmic extracts were stored at −80°C.

Extracts (25 μl) were treated with RNase A (160 μg/ml) at room temperature for 15 min and then adjusted to 5% β-mercaptoethanol, 8 M urea, 5% NP-40, and 2% ampholines, pH 5 to 8 (Bio-Rad), for an additional 15-min incubation preparatory to two-dimensional protein analyses (26, 47, 48). Samples were fractionated by isoelectric focusing in cylindrical gels (12 cm high by 0.4 cm in diameter) containing 4% polyacrylamide, 8 M urea, 2% NP-40, and 2% ampholines, pH 5 to 8. Volumes of cytoplasmic extract used for isoelectric focusing were 12.5 μl for samples for subsequent anti-3D analysis and 25 μl for subsequent antiuridine analysis. The top, alkaline, chamber contained 0.01 N NaOH, and the bottom, acidic, chamber contained 0.01 M phosphoric acid. Electrophoresis was at 340 V (constant) for at least 15 h, followed by 800 V for 1 h. The gels were collected into 2× SDS sample buffer. These gels were layered and sealed onto 10% polyacrylamide-SDS gels (16 cm wide by 12.5 cm long by 1.5 mm thick) with 0.7% agarose. Electrophoresis was performed at 180 V until the bromphenol blue dye front reached the bottom. The gels were blotted to nitrocellulose and treated sequentially with primary antibody (anti-3D or antiuridine serum), secondary antibody (anti-rabbit, alkaline phosphatase conjugate), and color reagents (NBT-BCIP) to detect immunoreactive proteins.

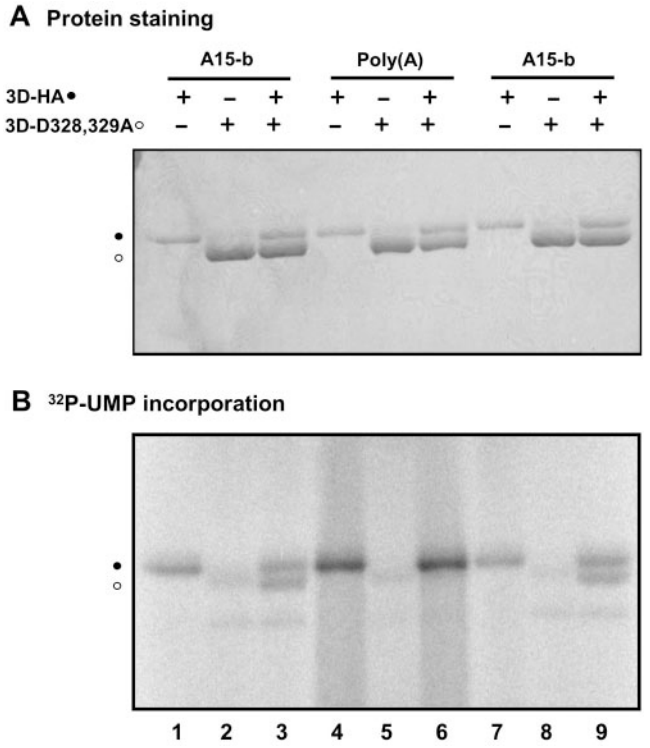

FIG. 2. Intra- and intermolecular uridylylation of 3D polymerase. Enzymatically active HA-tagged 3D polymerase (lanes 1, 4, and 7), enzymatically inactive 3D-D328/329A (lanes 2, 5, and 8), and mixtures of these two molecules (lanes 3, 6, and 9) were incubated under 3D uridylylation conditions with [^{32}P]UTP but without 3AB. Products were resolved in 10% polyacrylamide-SDS gels and analyzed (A) by protein staining, to detect both HA-tagged 3D and 3D-D328/329A, and (B) by autoradiography, to identify the uridylylated 3D species. The templates used for uridylylation reactions are indicated.

RESULTS

Uridylylation of 3D polymerase. Previous work has shown that poliovirus 3D polymerase catalyzes the formation of a phosphodiester linkage between a uridylate residue and the hydroxyl group on Tyr3 of viral protein VPg (3B) (18, 50–52). The resulting mono- and di-uridylylation of VPg is a prerequisite for initiation of viral RNA synthesis during the replication of poliovirus, as well as other picornaviruses (17, 33, 37, 39). The uridylylation reaction requires an RNA template to direct the addition of two uridylate residues to VPg. A small stem-loop structure located in the 2C coding region of poliovirus RNA (2C-*cre*), as well as poly(A), serve as efficient templates for uridylylation of poliovirus VPg in vitro. While exam-

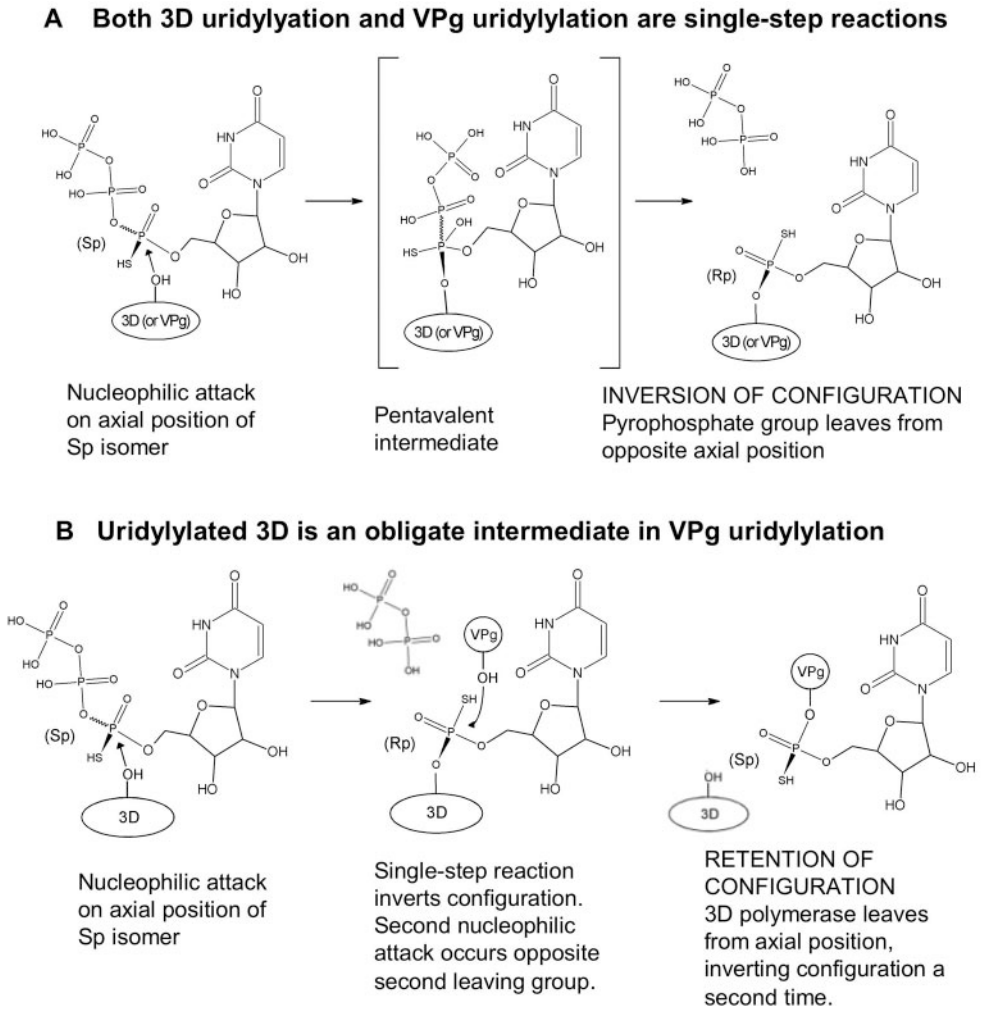

FIG. 3. Phosphate chirality can be used to determine whether uridylylation reactions are single-step reactions or proceed through covalent intermediates. (A) Expected chirality if the uridylylation of 3D polymerase and VPg uridylylation are single-step reactions. (B) Expected chirality if uridylylated 3D polymerase is an obligate intermediate in VPg uridylylation. Chirality is defined based on the priority of the groups in the chiral [(Sp)α-^{35}S]UTP.

ining the properties and parameters of poliovirus VPg uridylylation by highly purified 3D polymerase, we observed that the polymerase itself was also uridylylated in vitro under certain conditions. Figure 1A shows the products of in vitro uridylylation reactions that employed different adenylate homopolymers as templates. The templates were poly(A), which was on average 300 nt long, and oligonucleotides A15-b and A30-b, which were 15 and 30 adenyl residues, respectively, with blocked 3′ termini to prevent the addition of nontemplated nucleotides (45). Independent experiments showed that the time points used in this and subsequent experiments reflected initial rates of uridylylation (data not shown). As shown in Fig. 1A, uridylylation of the 22-amino-acid VPg peptide was favored with the poly(A) template in a reaction whose rate was only slightly affected by the addition of poliovirus protein 3AB (compare lanes 1 and 3). However, in the presence of the A15-b or A30-b template, 3D polymerase itself was uridylylated in reactions that were stimulated 10- to 25-fold by the presence of 3AB (lanes 6 and 7 and lanes 10 and 11). When other templates were tested, it was found that larger templates, such as poly(A) and 2C RNA, supported only very low amounts of 3D uridylylation. In the absence of any RNA template, a small but detectable amount of uridylylation of both the polymerase and VPg was observed (Fig. 1B). Therefore, both uridylylation reactions are strongly stimulated by the presence of RNA template, even one as small as A15-b, but are not absolutely dependent on template addition under these conditions. In summary, the choice of uridylylation substrate (VPg or 3D polymerase) and the rate of uridylylation were affected both by the presence of the known allosteric effector 3AB and by the presence and length of the RNA template.

Further characterization of the 3D polymerase uridylylation reactions, performed in the presence of the A15b template, is shown in Fig. 1C. The reaction showed maximal stimulation by 3AB at 4 μM 3AB (lane 3); at this 3AB concentration, uridylylated products continued to accumulate for 7 h at 30°C (lanes 8 to 13). The reaction displayed a broad pH maximum (pH 7 to 8) and an increased rate in the presence of Mn^{2+} compared

to Mg^{2+} and was stimulated by the presence of 2 mM DTT and 6 to 10% glycerol (data not shown).

Intermolecular and intramolecular uridylylation of 3D. To determine whether the uridylylation of 3D polymerase occurred intramolecularly, with the catalyst molecule using itself as a substrate, or intermolecularly, with one polymerase catalyzing UMP transfer to another, we tested whether catalytically active, epitope-tagged 3D polymerase (3D-HA) could uridylylate a catalytically inactive but untagged 3D polymerase (3D-D328A/D329A). Mutagenesis of the catalytic aspartates Asp328 and Asp329 has been shown to reduce RNA-dependent RNA elongation and VPg uridylylation activities to background levels (27, 35). Samples of the tagged, active polymerase and the 3D-D328A/D329A polymerase were incubated individually or together under uridylylation conditions, with either the poly(A) or A15-b template. To facilitate comparison of the RNA templates, these reactions were performed in the absence of 3AB so that the rates of the uridylylation reactions would be comparable, albeit very low (Fig. 1). As can be seen in the gel stained to detect total protein in Fig. 2A, HA-tagged 3D polymerase migrated more slowly in polyacrylamide-SDS gels than did the inactive mutant polymerase 3D-D328A/D329A, and the two polymerases could be readily distinguished when mixed. Figure 2B, an autoradiogram of the labeled, uridylylated proteins, shows that, in the presence of the A15-b template (lanes 1 to 3 and 7 to 9), both the active and the inactive polymerases were uridylylated in the presence of the active 3D-HA polymerase (lanes 3 and 9). Therefore, uridylylation of 3D polymerase can occur intermolecularly. With a poly(A) template, on the other hand, only active, HA-tagged 3D was efficiently labeled with [^{32}P]UMP (Fig. 2B, lanes 4 and 6). This finding is most consistent with the hypothesis that, in the presence of the longer template, intramolecular uridylylation is preferred, although some template-dependent event that sequesters the two kinds of polymerase from each other is also possible. The change from intermolecular uridylylation, observed with the A15-b template, to a potentially exclusively intramolecular uridylylation, observed with the poly(A) template, implies that large conformational changes in the polymerase occur as a function of template length.

Uridylylated 3D polymerase is not a required intermediate for uridylylation of VPg. To investigate whether uridylylated 3D polymerase was a necessary intermediate in VPg uridylylation, or vice versa, we monitored the chirality of the newly formed phosphodiester bonds in both uridylylated VPg and 3D polymerase. Phosphoryl transfer reactions occur by direct displacement, resulting in inversion of configuration of the phosphate (9, 13, 30). When a chiral substrate such as [(Sp)α-^{35}S]thio-UTP undergoes a single-step transesterification reaction, the end product has the opposite configuration (Rp) (Fig. 3A). Thus, if uridylylation of 3D polymerase or VPg occurs via a single-step reaction, the phosphate in the diester linkage between 3D polymerase or VPg and UMP will be converted to the Rp configuration. If, on the other hand, one of these substrates (for example, VPg) is uridylylated via an intermediate (for example, 3D polymerase-pU), then the final product, having undergone two inversions of configuration, will retain the original configuration of the chiral phosphate (Sp) (Fig. 3B).

We first examined the chirality of the phosphate in uridylylated 3D polymerase by using [(Sp)α-^{35}S]thio-UTP. The configuration of the phosphate in diester linkage to 3D polymerase was determined by its sensitivity to stereospecific nucleases. Cleavage by SVPD cleaves only Rp phosphorothioate diesters (8); thus, removal of the labeled uridylyl moiety from 3D polymerase by this enzyme would indicate a single-step reaction (Fig. 4A). On the other hand, if formation of uridylylated 3D polymerase occurred through a covalent intermediate, the product would have the Sp configuration and display resistance to SVPD (Fig. 4B). Experimentally, the products of

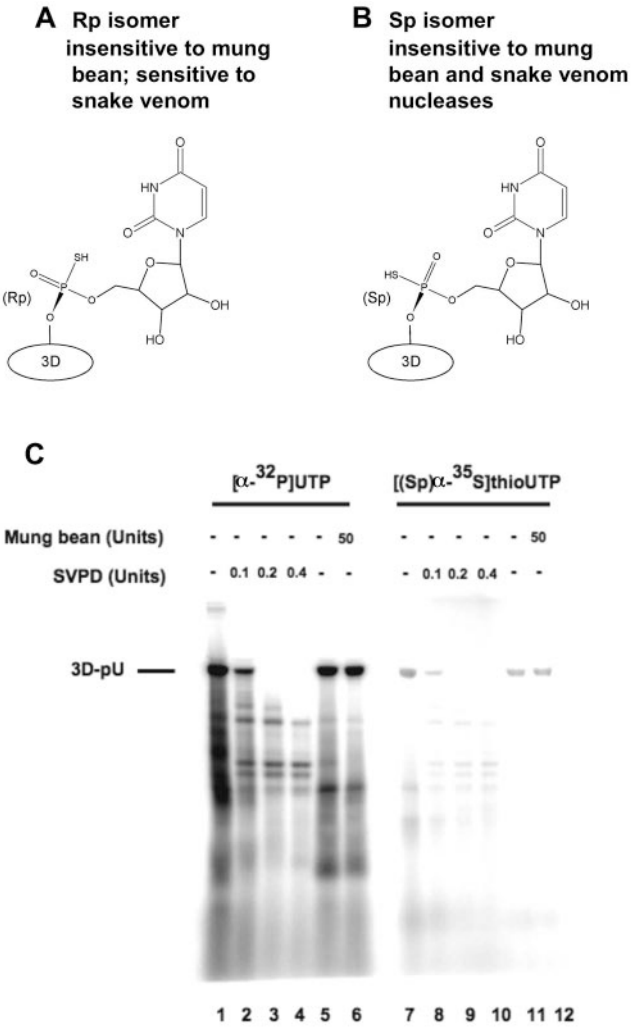

FIG. 4. Chirality of uridylylation of 3D. (A) Formation of a 3D uridylylation product containing a chiral phosphate diester linkage (3D polymerase to UMP) of the Rp configuration is susceptible to SVPD cleavage (specific for Rp chiral phosphate). (B) Formation of a 3D polymerase uridylylation product with a chiral phosphate diester linkage of the Sp configuration is not cleavable by SVPD. (C) Uridylylation of 3D polymerase was performed as described in Materials and Methods with 10 μM A15-b template, 3 μM 3AB, 2 μM [^{32}P]UTP, and 2 μM 3D at 30°C for 60 min (lanes 1 to 6) or with A15-b, 3AB, 3D, and 0.9 μM [(Sp)α-^{35}S]UTP at 30°C for 180 min (lanes 7 to 12). Products were treated with SVPD or mung bean nuclease (Sp-specific cleavage) at the indicated concentrations, followed by RNase A digestion, as described in Materials and Methods. Products were resolved in 12% polyacrylamide-Tris-Tricine gels and analyzed by autoradiography.

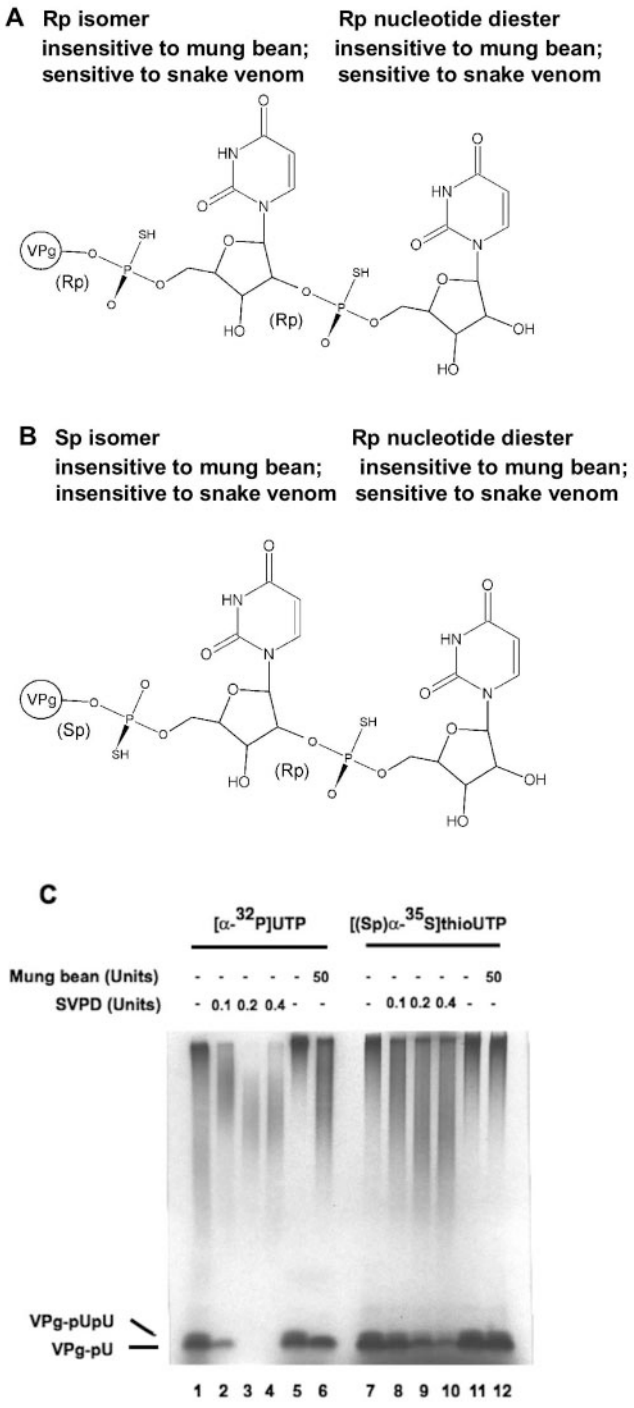

FIG. 5. Chirality of uridylylation of VPg. (A) Formation of a VPg uridylylation product may produce VPg-pU or VPg-pUpU. If the diester linkage between VPg and UMP is in the Rp configuration, it is susceptible to cleavage by Rp-specific SVPD. It is predicted that the internucleotide linkage would be a single-step reaction, thus of the Rp configuration and, therefore, susceptible to cleavage by SVPD. In both cases the bonds would not be susceptible to mung bean nuclease cleavage (Sp-specific enzyme). (B) If formation of the linkage between VPg and UMP goes through an intermediate, that chiral phosphate would have the Sp configuration and hence not be susceptible to SVPD cleavage but still not cleavable by mung bean nuclease (requires internucleotide linkage; resistant to a mixed diester linkage). However, the internucleotide linkage remains, as in panel A, and hence is susceptible to SVPD only. (C) Uridylylation of VPg was performed as described in Materials and Methods and includes 1 μM poly(A) template, 50 μM VPg, 2 μM [^{32}P]UTP, and 2 μM 3D polymerase, incubated at 30°C for 60 min (lanes 1 to 6), or with poly(A), VPg, 3D polymerase, and 0.9 μM [(Sp)α-^{35}S]UTP at 30°C for 180 min (lanes 7 to 12). Products were treated as described in the legend to Fig. 4 but without RNase A digestion, resolved in 12% polyacrylamide-Tris-Tricine gels, and analyzed by autoradiography. The labeled material at the top of the lanes is end-labeled poly(A) template used in these VPg uridylylation reactions; 3D polymerase is known to catalyze terminal uridylylation of unblocked RNA molecules (45).

two uridylylation reactions were examined for susceptibility to both SVPD and mung bean nuclease (Fig. 4C). As a control, 3D polymerase was uridylylated with [α-^{32}P]UTP, which has a nonchiral α-phosphate, and the product was digested with a series of concentrations of SVPD (lanes 2 to 4), showing that the enzyme is active in removing the nonchiral [^{32}P]5′-UMP. When the product was treated with mung bean nuclease (lane 6), we found that this nuclease was not capable of cleaving the mixed diester. We concluded that mung bean nuclease is able to cleave only internucleotide Sp diesters and would therefore not be useful in determining the chirality of the UMP-protein linkage. When 3D polymerase was uridylylated with [(Sp)α-^{35}S]thio-UTP, the labeled, chiral UMP moiety could be removed by digestion with SVPD (Fig. 4C, lanes 8 to 10). Therefore, the 3D polymerase-UMP bond was in the Rp configuration, arguing that the uridyl moiety was added to 3D polymerase from [(Sp)α-^{35}S]thio-UTP, and presumably UTP, via a single-step reaction.

We next explored whether uridylylated 3D polymerase served as an obligate intermediate in VPg uridylylation. If addition of the first UMP to VPg occurred by single-step, direct transfer, a chiral phosphate between VPg and uridine would have the Rp configuration and would therefore be sensitive to SVPD (Fig. 5A); it would not be sensitive to mung bean nuclease. Furthermore, if VPg-pU were subsequently uridylylated to VPg-pUpU, we would predict that this would be a direct addition of UMP and thus an Rp diester. This internucleotide bond would be predicted to be susceptible to SVPD, because it was Rp, and insensitive to mung bean nuclease, because even though it is a nucleotide diester, mung bean nuclease cleaves only internucleotide diesters of the Sp configuration (Fig. 5A). If VPg uridylylation, on the other hand, were catalyzed via a covalent intermediate such as uridylylated 3D polymerase, then the first VPg-uridine linkage would have an Sp configuration and would not be cleaved by SVPD and the second would be sensitive to SVPD and insensitive to mung bean nuclease (Fig. 5B).

To test the chirality of the VPg-pUpU diester bonds, VPg was uridylylated in the presence of 3D polymerase and either nonchiral [^{32}P]UTP (Fig. 5C, lanes 1 to 6) or chiral [(Sp)α-^{35}S]thio-UTP (lanes 7 to 12). With the nonchiral ^{32}P-labeled product, the ^{32}P label was completely removed by SVPD, as expected (lanes 2 to 4). Mung bean nuclease treatment, on the other hand, removed only the internucleotide bond, converting VPg-pUpU to VPg-pU (lanes 5 and 6), confirming that mung bean nuclease cleavage requires an internucleotide linkage. With the chiral substrate, [(Sp)α-^{35}S]thio-UTP, at least 75% of

the ^{35}S in VPg-pU was removed by SVPD, arguing that most of the VPg-pU bond was present in the Rp configuration and therefore the uridylylation occurred by a single step. In repeated experiments there was always a small amount of residual uncleaved VPg-pU linkage, suggesting either a failure to completely cleave the residual VPg-pU or the presence of a small amount of product from a two-step reaction. Thus, under the conditions of the experiment, VPg uridylylation occurred predominantly by single-step, direct transfer of the uridylate moiety, without using uridylylated 3D polymerase as an intermediate. Neither linkage was cleaved by mung bean nuclease, confirming that mixed diesters are not cleaved by this enzyme and that the second uridylate moiety added was also added by a single step, with the resulting Rp internucleotide bond being insensitive to mung bean nuclease.

The 3D uridylylation product, as has been reported for the VPg uridylylation product (15, 46), was found to be stable to digestion with alkaline phosphatase, to boiling in the presence of 1% SDS, and to electrophoresis. As discussed above, the sensitivity of the product to digestion with SVPD (Fig. 4 and 5) indicates the presence of a diester linkage. A lack of effect of mung bean nuclease (Fig. 4C) or RNase A (data not shown) on uridylylated 3D polymerase suggests that, at most, two UMP moieties were added at any given site. By calculating the amount of ^{32}P incorporated and assuming one uridylylation site per 3D polymerase molecule, we found that in reactions such as that shown in Fig. 1A (lanes 6 and 7), the extent of uridylylation of 3D polymerase with labeled UTP varied from 10% to 20%. Thus far, all active mutant and variant 3D polymerases have displayed similar efficiencies of uridylylation in solution, including coxsackievirus 3D polymerase and mutant poliovirus polymerases 3D-R455D and 3D-D349R (data not shown). Direct attempts to determine the percentage of uridylylated 3D polymerase, and to identify the modified peptide or peptides by mass spectrometry, have been unsuccessful. We presume that uridylylated peptides, like phosphorylated peptides, display low ionization efficiencies, and their detection will require biochemical enrichment before mass spectrometry (reviewed in reference 57).

Other poliovirus proteins can be uridylylated by 3D polymerase. The 3D protein sequences are also present as part of a larger polypeptide, 3CD, that accumulates during poliovirus infection and has specific functions distinct from 3D polymerase. We tested whether purified 3CD protein could serve as a substrate for uridylylation by active 3D polymerase. The protease active site of 3CD was mutated (C147A) to prevent intramolecular cleavage. Purified viral proteins 3D and 3CD were incubated in the presence of A15-b and [^{32}P]UTP, subjected to electrophoresis in a 10% polyacrylamide-SDS gel, blotted to nitrocellulose, and analyzed by autoradiography (Fig. 6). As shown in Fig. 1, uridylylation of 3D polymerase was substantially stimulated by 3AB (compare lanes 1 and 2). Protein 3CD was uridylylated in the presence of 3D polymerase (lane 4), and this reaction was also amplified by the addition of 3AB (lane 3). The presence of 3CD slightly decreased the rate of 3D uridylylation compared to that of 3D polymerase alone (compare lane 4 to lane 1). Protein 3CD alone, 3AB alone, or 3CD in the presence of 3AB gave no measurable signal (data not shown). Therefore, 3AB binding to either 3D polymerase or 3CD protein renders 3CD a suitable substrate for intermolecular uridylylation by 3D polymerase.

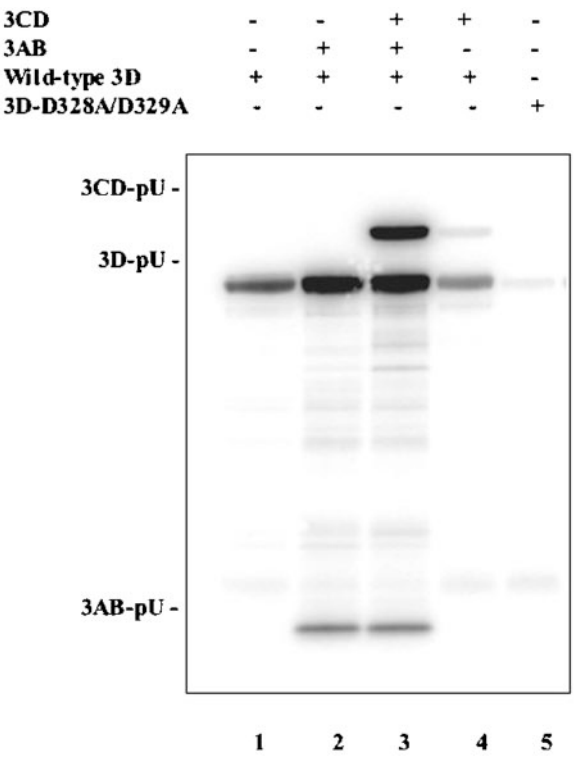

FIG. 6. Intermolecular uridylylation of 3CD and 3AB by 3D polymerase. Uridylylation reactions were as described in Materials and Methods with 10 μM A15-b, 5 μM UTP (5 μCi/30 μl), 1 μM 3D polymerase, and 1 μM 3CD and/or 5 μM 3AB, as indicated. Incubations were at 30°C for 2 h; products were digested with RNase A, heated at 90°C in sample buffer, and resolved in 10% polyacrylamide-SDS gels. The autoradiogram illustrates the presence of 3D-pU, 3CD-pU, and 3AB-pU.

Poliovirus protein 3AB, long thought to be the nonuridylylatible precursor of VPg (32, 53), was also found to be uridylylated by 3D polymerase, using the short A15b template, in the presence or absence of 3CD protein (Fig. 6). Visualization of 3AB was facilitated in this experiment, compared to that shown in Fig. 1, due to the use of a 12% Tricine gel in the experiment represented in Fig. 1 and more standard electrophoresis conditions in that of Fig. 6 (see Materials and Methods). However, in retrospect, inspection of Fig. 1B reveals the presence of uridylylated 3AB migrating halfway down the gel. Thus, the viral substrates of uridylylation by 3D polymerase are 3D polymerase, in both intramolecular and intermolecular reactions, 3CD, 3AB, and, as has been reported previously, the protein primer VPg (3B).

Purified 3D polymerase is uridylylated in *E. coli*, and a HeLa cell protein is uridylylated in the absence of viral infection. We do not yet know the function of intramolecular or intermolecular uridylylation of 3D polymerase, but its template dependence caused us to wonder whether 3D polymerase expressed in *E. coli* was subject to uridylylation in the bacterial intracellular environment. To test this, we obtained antiuridine antibodies to test the presence of uridine moieties in unlabeled

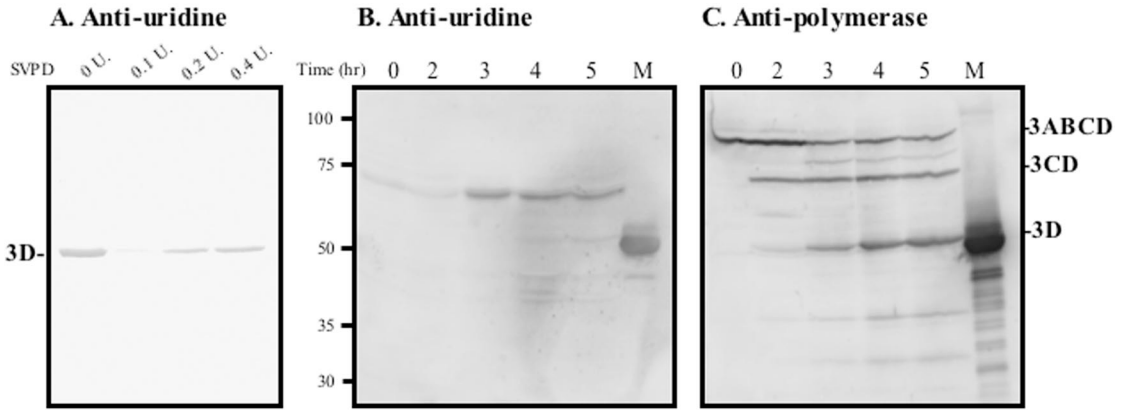

FIG. 7. Monitoring of protein uridylylation with an antiuridine antibody. (A) Purified 3D is already uridylylated. 3D purified from *E. coli* extracts was denatured and treated with SVPD at the indicated levels (lanes 2 to 4); untreated 3D is shown in lane 1. Products were fractionated in a 10% polyacrylamide-SDS gel and blotted to nitrocellulose, and immunoreactive species were detected by immunoblotting (7) with antiuridine serum, as described in Materials and Methods. (B and C) Time course of appearance of immunoreactive species in soluble cytoplasmic extracts derived from poliovirus-infected HeLa cells (see Materials and Methods). (B) Appearance of antiuridine reactive proteins with time. The 3D marker is indicated. (C) Appearance of anti-3D reactive species with time. Again, the 3D marker is indicated. In both B and C, proteins were blotted to PVDF membranes and were detected with the ECF reagent (Amersham).

proteins isolated from cells. As shown in Fig. 7A, purified wild-type poliovirus 3D polymerase, isolated from *E. coli*, was immunoreactive with antiuridine serum in immunoblot analysis (lane 1). That this signal reflected the presence of a uridine moiety in diester linkage to the protein was confirmed by its removal upon incubation with a low concentration of SVPD (lanes 2 to 4). At higher concentrations of SVPD, we noted incomplete removal of the uridylate moiety, most likely due to higher concentrations of glycerol in the incubations. The uridylylation of 3D polymerase in *E. coli* appears to be accomplished by a bacterial enzyme, because catalytically inactive 3D-D328A/D329A was also uridylylated to approximately the same extent upon purification (data not shown).

The availability of antiuridine antibody prompted us to search for uridylylated species in poliovirus-infected cells. To this end, cytoplasmic extracts prepared from HeLa cells at various times postinfection with poliovirus were analyzed with antiuridine (Fig. 7B) and antipolymerase (Fig. 7C) antibodies. Interestingly, a host protein, migrating slightly faster than poliovirus 3CD, was found to be immunoreactive with the antiuridine antibody (Fig. 7B, lanes 3 to 5 h postinfection). As a small amount of this protein was found to be uridylylated before the beginning of poliovirus infection (see 0-h point, Fig. 7B), we do not know whether the increased uridylylation observed during poliovirus infection was due to the enzymatic action of poliovirus 3D polymerase or not. The mobilities of poliovirus proteins 3D, 3CD, and the higher-molecular-weight precursor 3ABCD (P3) can be seen in Fig. 7C; in the one-dimensional gel shown in Fig. 7B, it was difficult to ascertain whether or not these species were uridylylated.

Uridylylated 3D and 3CD are present in poliovirus-infected HeLa cells. To search more carefully for uridylylated forms of poliovirus 3D, 3CD, or other 3D-containing polypeptides in cytoplasmic extracts of poliovirus-infected cells, we employed two-dimensional protein analyses. Extracts of cells infected with mutant poliovirus 3D-111 (12) were analyzed by two-dimensional electrophoresis (26, 47, 48). The 3D-111 mutant virus, despite the presence of two amino acid changes in the 3D polymerase coding region (E98A/D99A), displays wild-type growth characteristics. These two mutations, however, alter the electrophoretic mobilities of the 3D-containing proteins (12), which facilitated their identification in the two-dimensional separations. The first dimension of the electrophoretic analysis was isoelectric focusing in cylindrical gels (pH 5 to 8), followed by analysis of each tube gel in 10% polyacrylamide-SDS. Proteins were blotted to nitrocellulose and analyzed for anti-3D polymerase and antiuridine immunoreactive species (Fig. 8).

In extracts from infected cells, several protein species were found to react with the anti-3D polymerase antibody. In poliovirus-infected cells, alternative cleavage products of 3CD, 3C′ and 3D′, are known to form in addition to 3CD and 3D polymerase; 3C′ contains all 3C sequences and 148 amino acids from the amino terminus of 3D polymerase, and 3D′ consists of the 313 C-terminal residues of 3D (11, 20, 56). All of these polypeptides were detected with an antipolymerase polyclonal antibody (Fig. 8, bottom right panel). In contrast, an anti-3D blot of extracts from mock-infected cells (bottom left) lacked these characteristic spots of poliovirus proteins, revealing instead a few background spots. Analysis of a blot from poliovirus-infected cells with antiuridine (top right) showed a single spot that corresponds to 3D polymerase, as well as faint spots that correspond to both 3CD and 3C′. No antiuridine staining that corresponds to 3D′ was observed (Fig. 8). Similar results by two-dimensional gel analysis were obtained with extracts of cells infected with either wild-type or 3D-111 virus (data not shown). Therefore, several protein species that contain 3D-derived sequences—3CD, 3C′, and 3D polymerase itself—contain uridyl residues in poliovirus-infected cells. In addition, a host protein of approximately 65 to 70 kDa in size was found to contain uridyl moieties in uninfected cells, but its abundance, its uridylylation, or both increased during poliovirus infection.

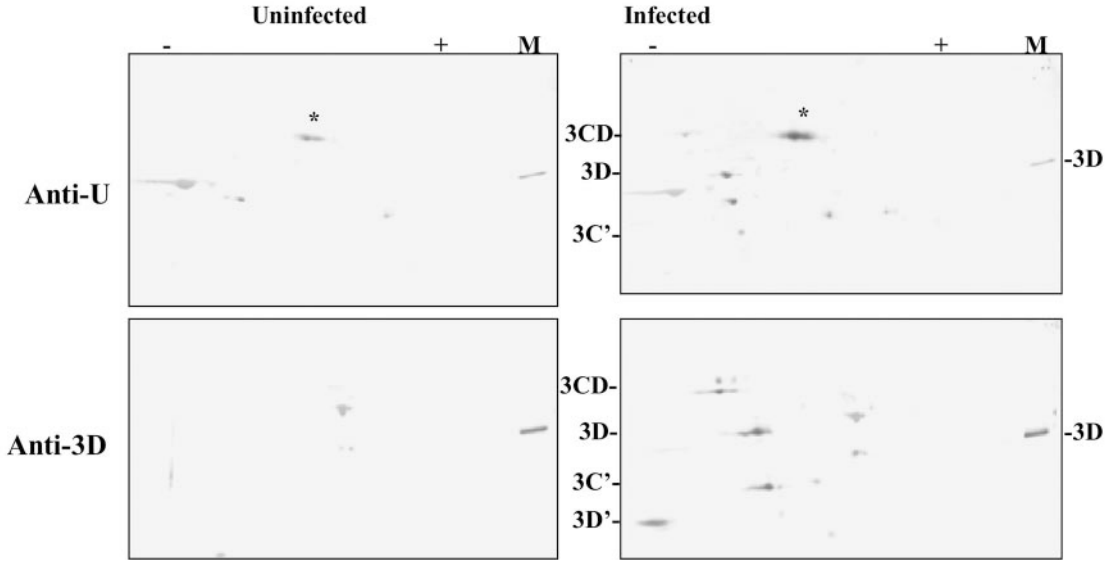

FIG. 8. Two-dimensional gel analysis of poliovirus (3D-111)-infected and mock-infected cytoplasmic extracts. Extracts were obtained from uninfected or poliovirus-infected HeLa cells, as described in Materials and Methods. These extracts were fractionated by isoelectric focusing, pH 5 to 8, in the first dimension, followed by 10% polyacrylamide-SDS fractionation in the second dimension. After the second dimension, gels were blotted to nitrocellulose and analyzed by Western immunoblot analyses with polyclonal anti-3D or polyclonal antiuridine, as indicated. The color detection system used NBT-BCIP (Promega). An asterisk denotes the uridylylated host protein in the antiuridine panels.

DISCUSSION

A functional role for the posttranslational uridylylation of certain cellular proteins is well documented. In the cascade of activation steps for glutamine synthetase, for example, the activity of P_{II} protein is controlled by its degree of uridylylation, which in turn controls glutamine synthetase activity (1, 28). Furthermore, the interconversion of galactose-1-phosphate and glucose-1-phosphate occurs in their uridylylated forms, using uridylyl transferase as a covalent intermediate (5, 16). In the P_{II} protein, a tyrosine residue serves as the acceptor for the uridylate residue (1, 59), whereas with uridyl transferase in galactose metabolism, a histidine is the uridylate acceptor (64).

Several years ago, Paul et al. (50) discovered that 3D polymerase, in the presence of a poly(A) template, could catalyze the uridylylation of viral protein VPg (3B); a tyrosine hydroxyl located near the N terminus of that protein was shown to be the acceptor in vitro. The present work describes additional protein acceptors for 3D polymerase-catalyzed nucleotide transfer. First, we observed that the 3D polymerase sequences themselves can serve as uridylate acceptors (Fig. 1). We have not yet determined the amino acid residue or residues of 3D polymerase that can be uridylylated. In the presence of poly(A), the uridylylation of poliovirus 3D polymerase was found to be intramolecular (Fig. 2), whereas in the presence of a shorter template, A15-b, 3D uridylylation was found to occur intermolecularly (Fig. 2) and was highly stimulated by the presence of viral protein 3AB (Fig. 1). Another viral protein that contains 3D sequences, 3CD, can also serve as a uridylate acceptor; this reaction was also greatly stimulated by 3AB and was more readily observed in the presence of a small RNA template such as A15-b. A 15-nt single-stranded RNA molecule is expected to bind to a single polymerase molecule, whereas longer RNA molecules have the capacity to bind multiple polymerases cooperatively (6). It is likely, therefore, that a conformational change in the polymerase that occurs upon multimerization (25, 36) can alter the substrate specificity of the uridylylation reaction. With small RNA templates, viral protein 3AB, a larger VPg-containing protein, was also observed to be uridylylated (Fig. 6). Thus, it is possible that, as in encephalomyocarditis virus (A. Palmenberg, personal communication), larger VPg-containing molecules could function as protein primers during viral RNA synthesis, especially early in infection when polymerase concentrations are low.

When poliovirus-infected HeLa cell extracts were examined for evidence of uridylylated forms of 3D proteins, both uridylylated 3D polymerase and 3CD protein were found (Fig. 8). Whether this unusual protein modification plays any role in the virus replication cycle is still unknown. However, the phosphate chirality experiments reported here exclude the possibility that uridylylated 3D polymerase molecules are obligate intermediates in the formation of uridylylated VPg, because both reactions were shown to occur via single biochemical steps (Fig. 4 and 5).

Two additional uridylylated proteins were found to accumulate in poliovirus-infected cells. A host protein, found to react with antiuridine antibody in extracts of uninfected cells, was found to increase in abundance, uridylylation state, or both during poliovirus infection (Fig. 7 and 8). Efforts are ongoing to identify this protein and determine its site of uridylylation in infected and uninfected cells. An alternative viral cleavage product, 3C′, which contains 3C sequences as well as 148 amino acids from the N terminus of 3D polymerase (20, 56), was found to be uridylylated in poliovirus-infected cells, whereas 3D′, which contains the C-terminal 313 amino acids of 3D polymerase, was not (Fig. 8). Therefore, assuming that the uridylylation site or sites in 3C′ are the same as those in 3CD

and 3D polymerase, it is likely that uridylylation of 3D-containing proteins occurs in the first 148 amino acids of the 3D sequence. This is a very flexible region of the protein that has crystallized in several different conformations (21, 24, 62) and forms the intramolecular connection between the "finger" and "thumb" domains of the polymerase (62). Experiments aimed at gaining an understanding of the structural and biochemical specificities of inter- and intramolecular uridylylation reactions catalyzed by poliovirus polymerase are ongoing.

ACKNOWLEDGMENTS

We thank Ellie Ehrenfeld for supporting this work in its initial stages and for numerous helpful suggestions. We thank Ellie Ehrenfeld and Peter Sarnow for critical readings of the manuscript, Chad Moore for help with phosphate stereochemistry, and Ann Dvorak and David Warmflash for providing antiuridine antibodies.

This work was supported by NIH grants AI-42119 (to K.K.) and GM 54194 (to R.D.K.).

REFERENCES

1. **Adler, S. P., D. Purich, and E. R. Stadtman.** 1975. Cascade control of *Escherichia coli* glutamine synthetase. Properties of the P_{II} regulatory protein and the uridylyltransferase-uridylyl removing enzyme. J. Biol. Chem. **16:**6264–6279.
2. **Andino, R., G. E. Rieckhof, and D. Baltimore.** 1990. A functional ribonucleoprotein complex forms around the 5′-end of poliovirus RNA. Cell **63:**369–380.
3. **Andino, R., G. E. Rieckhof, P. L. Achacoso, and D. Baltimore.** 1993. Poliovirus RNA synthesis utilizes an RNP complex formed around the 5′-end of viral RNA. EMBO J. **12:**3587–3598.
4. **Ansardi, D. C., D. C. Porter, and C. D. Morrow.** 1992. Myristoylation of poliovirus capsid precursor P1 is required for assembly of subviral particles. J. Virol. **66:**4556–4563.
5. **Arabshahi, A., R. S. Brody, A. Smallwood, T.-C. Tsai, and P. A. Frey.** 1986. Galactose-1-phosphate uridylyltransferase. Purification of the enzyme and stereochemical course of each step of the double-displacement mechanism. Biochemistry **25:**5583–5589.
6. **Beckman, M. T. L., and K. Kirkegaard.** 1998. Site size of cooperative single-stranded RNA binding by poliovirus RNA-dependent RNA polymerase. J. Biol. Chem. **273:**6724–6730.
7. **Blake, M. S., K. H. Johnston, G. I. Russell-Jones, and E. C. Gotschlich.** 1984. A rapid, sensitive method for detection of alkaline phosphatase-conjugated anti-antibody on Western blots. Anal. Biochem. **136:**175–179.
8. **Bryant, F. R., and S. J. Benkovic.** 1978. Stereochemical course of the reaction catalyzed by 5′-nucleotide phosphodiesterase from snake venom. Biochemistry **18:**2825–2828.
9. **Buchwald, S. L., D. E. Hansen, A. Hassett, and J. R. Knowles.** 1982. Chiral [16O, 17O, 18O] phosphoric monoesters as stereochemical probes of phosphotransferases. Methods Enzymol. **87:**279–301.
10. **Dayhuff, T. J., R. F. Gesteland, and J. F. Atkins.** 1992. Electrophoresis, autoradiography and electroblotting of peptides: T4 gene 60 hopping. BioTechniques **13:**500–503.
11. **Dewalt, P. G., and B. L. Semler.** 1989. Molecular biology and genetics of poliovirus protein processing, p. 73–93. *In* B. L. Semler and E. Ehrenfeld (ed.), Molecular aspects of picornavirus infection and detection. American Society for Microbiology, Washington, D.C.
12. **Diamond, S. E., and K. Kirkegaard.** 1994. Clustered charged-to-alanine mutagenesis of poliovirus RNA-dependent RNA polymerase yields multiple temperature-sensitive mutants defective in RNA synthesis. J. Virol. **68:**863–876.
13. **Eckstein, F.** 1985. Nucleoside phosphorothioates. Annu. Rev. Biochem. **54:**367–402.
14. **Ferrer-Orta, C., A. Arias, R. Perez-Luque, C. Escarmis, E. Domingo, and N. Verdaguer.** 2004. Structure of foot-and-mouth disease virus RNA-dependent RNA polymerase and its complex with a template-primer RNA. J. Biol. Chem. **279:**47212–47221.
15. **Flanegan, J. B., R. F. Pettersson, V. Ambros, M. J. Hewlett, and D. Baltimore.** 1977. Covalent linkage of a protein to a defined nucleotide sequence at the 5′-terminus of virion and replicative intermediate RNAs of poliovirus. Proc. Natl. Acad. Sci. USA **74:**961–965.
16. **Geeganage, S., and P. A. Frey.** 1998. Transient kinetics of formation and reaction of the uridylyl-enzyme form of galactose-1-P uridylyltransferase and its Q168R-variant: insight into the molecular basis of galactosemia. Biochemistry **37:**14500–14507.
17. **Gerber, K., E. Wimmer, and A. V. Paul.** 2001. Biochemical and genetic studies of the initiation of human rhinovirus 2 RNA replication: identification of a *cis*-replication element in the coding sequence of $2A^{pro}$. J. Virol. **75:**10979–10990.
18. **Goodfellow, I., Y. Chaudhry, A. Richardson, J. Meredith, J. W. Almond, W. Barclay, and D. J. Evans.** 2000. Identification of a *cis*-acting replication element within the poliovirus coding region. J. Virol. **74:**4590–4600.
19. **Goodfellow, I. G., C. Polacek, R. Andino, and D. J. Evans.** 2003. The poliovirus 2C cis-acting replication element-mediated uridylylation of VPg is not required for synthesis of negative-sense genomes. J. Gen. Virol. **84:**2359–2363.
20. **Hanecak, R., B. L. Semler, C. W. Anderson, and E. Wimmer.** 1982. Proteolytic processing of poliovirus polypeptides: antibodies to polypeptide P3-7c inhibit cleavage of glutamine-glycine pairs. Proc. Natl. Acad. Sci. USA **79:**3973–3977.
21. **Hansen, J. L., A. M. Long, and S. C. Schultz.** 1997. Structure of the RNA-dependent RNA polymerase of poliovirus. Structure **5:**1109–1122.
22. **Harris, K. S., S. R. Reddigari, M. J. Nicklin, T. Hammerie, and E. Wimmer.** 1992. Purification and characterization of poliovirus polypeptide 3CD, a proteinase and a precursor for RNA polymerase. J. Virol. **66:**7481–7489.
23. **Harris, K. S., W. Xiang, L. Alexander, W. S. Lane, A. V. Paul, and E. Wimmer.** 1994. Interaction of poliovirus polypeptide 3CDpro with the 5′ and 3′ termini of the poliovirus genome. Identification of viral and cellular cofactors needed for efficient binding. J. Biol. Chem. **269:**27004–27014.
24. **Hobson, S. D.** 2000. Crystallographic and biochemical studies of higher order poliovirus polymerase structures. Ph.D. thesis. University of Colorado, Boulder, Colo.
25. **Hobson, S. D., E. S. Rosenblum, O. C. Richards, K. Richmond, K. Kirkegaard, and S. C. Schultz.** 2001. Oligomeric structures of poliovirus polymerase are important for function. EMBO J. **20:**1153–1163.
26. **Hochstrasser, D. F., M. G. Harrington, A.-C. Hochstrasser, M. J. Miller, and C. R. Merril.** 1988. Methods for increasing the resolution of two-dimensional protein electrophoresis. Anal. Biochem. **173:**424–435.
27. **Jablonski, S. A., and C. D. Morrow.** 1995. Mutation of the aspartic acid residues of the GDD sequence motif of poliovirus RNA-dependent RNA polymerase results in enzymes with altered metal ion requirements for activity. J. Virol. **69:**1532–1539.
28. **Jiang, P., P. Zucker, M. R. Atkinson, E. S. Kamberov, W. Tirasophon, P. Chandran, B. R. Schefke, and A. J. Ninfa.** 1997. Structure/function analysis of the P_{II} signal transduction protein of *Escherichia coli*: genetic separation of interactions with protein receptors. J. Bacteriol. **179:**4342–4353.
29. **Jore, J., B. DeGeus, R. J. Jackson, P. H. Pouwels, and B. E. Enger-Valk.** 1988. Poliovirus protein 3CD is the active protease for processing of the precursor protein P1 *in vivo*. J. Gen. Virol. **69:**1627–1636.
30. **Knowles, J. R.** 1980. Enzyme-catalyzed phosphoryl transfer reactions. Annu. Rev. Biochem. **49:**877–919.
31. **Lama, J., and L. Carrasco.** 1992. Inducible expression of a toxic poliovirus membrane protein in *Escherichia coli*: comparative studies using different expression systems based on T7 promoter. Biochem. Biophys. Res. Commun. **188:**972–981.
32. **Lama, J., A. V. Paul, K. S. Harris, and E. Wimmer.** 1994. Properties of purified recombinant poliovirus protein 3AB as substrate for viral proteinases and as cofactor for RNA polymerase 3D polymerase. J. Biol. Chem. **269:**66–70.
33. **Lobert, P.-E., N. Escrion, J. Ruelle, and T. Michiels.** 1999. A coding RNA sequence acts as a replication signal in cardioviruses. Proc. Natl. Acad. Sci. USA **96:**11560–11565.
34. **Love, R. A., K. A. Maegley, X. Yu, R. A. Ferre, L. K. Lingardo, W. Diehl, H. E. Parge, P. S. Dragovich, and S. A. Fuhrman.** 2004. The crystal structure of the RNA-dependent RNA polymerase from human rhinovirus. A dual function target for common cold antiviral therapy. Structure **12:**1533–1544.
35. **Lyle, J. M., A. Clewell, K. Richmond, O. C. Richards, D. A. Hope, S. C. Schultz, and K. Kirkegaard.** 2002. Similar structural basis for membrane localization and protein priming by RNA-dependent RNA polymerase. J. Biol. Chem. **277:**16324–16331.
36. **Lyle, J. M., E. Bullitt, K. Bienz, and K. Kirkegaard.** 2002. Visualization and functional analysis of RNA-dependent RNA polymerase lattices. Science **296:**2218–2222.
37. **Mason, P. W., S. V. Bezboradova, and T. M. Henry.** 2002. Identification and characterization of a *cis*-acting replication element (*cre*) adjacent to the internal ribosome entry site of foot-and-mouth disease virus. J. Virol. **76:**9686–9694.
38. **McKnight, K. L., and S. M. Lemon.** 1996. Capsid coding sequence is required for efficient replication of human rhinovirus 14. J. Virol. **70:**1941–1952.
39. **McKnight, K. L., and S. M. Lemon.** 1998. The rhinovirus type 14 genome contains an internally located RNA structure that is required for viral replication. RNA **4:**1569–1584.
40. **Moras, D.** 1993. Two sisters and their cousins. Nature **364:**572–573.
41. **Morasco, B. J., N. Sharma, J. Parilla, and J. B. Flanegan.** 2003. Poliovirus *cre*(2C)-dependent synthesis of VpgpUpU is required for positive- but not negative-strand RNA synthesis. J. Virol. **77:**5136–5147.
42. **Moscufo, N., A. G. Yafal, A. Rogove, J. Hogle, and M. Chow.** 1993. A

mutation in VP4 defines a new step in the late stages of cell entry by poliovirus. J. Virol. **67:**5075–5078.
43. **Murray, K. E., and D. J. Barton.** 2003. Poliovirus CRE-dependent VPg uridylylation ts required for positive-strand RNA synthesis but not for negative-strand RNA synthesis. J. Virol. **77:**4739–4750.
44. **Nayak, A., I. G. Goodfellow, and G. J. Belsham.** 2005. Factors required for the uridylylation of the foot-and-mouth disease virus 3B1, 3B2, and 3B3 peptides by the RNA-dependent RNA polymerase ($3D^{pol}$) in vitro. J. Virol. **79:**7698–7706.
45. **Neufeld, K. L., J. M. Galarza, O. C. Richards, D. F. Summers, and E. Ehrenfeld.** 1994. Identification of terminal adenylyl transferase activity of the poliovirus polymerase $3D^{pol}$. J. Virol. **68:**5811–5818.
46. **Nomoto, A., B. Detjen, R. Pozzatti, and E. Wimmer.** 1977. The location of the polio genome protein in viral RNAs and its implication for RNA synthesis. Nature **268:**208–213.
47. **O'Farrell, P. H.** 1975. High resolution two-dimensional electrophoresis of proteins. J. Biol. Chem. **250:**4007–4021.
48. **O'Farrell, P. Z., H. M. Goodman, and P. H. O'Farrell.** 1977. High resolution two-dimensional electrophoresis of basic as well as acidic proteins. Cell **12:**1133–1142.
49. **Parsley, T. B., J. S. Towner, L. B. Blyn, E. Ehrenfeld, and B. L. Semler.** 1997. Poly(rC) binding protein 2 forms a ternary complex with the 5′-terminal sequences of poliovirus RNA and the viral 3CD proteinase. RNA **3:**1124–1134.
50. **Paul, A. V., J. H. von Boom, D. Fillippov, and E. Wimmer.** 1998. Protein-primed RNA synthesis by purified poliovirus RNA polymerase. Nature **393:**280–284.
51. **Paul, A. V., E. Rieder, D. W. Kim, J. H. von Boom, and E. Wimmer.** 2000. Identification of an RNA hairpin in poliovirus RNA that serves as the primary template in the in vitro uridylylation of VPg. J. Virol. **74:**10359–10370.
52. **Paul, A. V., J. Peters, J. Mugavero, J. Yin, J. H. von Boom, and E. Wimmer.** 2003. Biochemical and genetic studies of the VPg uridylylation reaction catalyzed by the RNA polymerase of poliovirus. J. Virol. **77:**891–904.
53. **Plotch, S. J., and O. Palant.** 1995. Poliovirus protein 3AB forms a complex with and stimulates the activity of the viral RNA polymerase, $3D^{pol}$. J. Virol. **69:**7169–7179.
54. **Ranjith-Kumar, C. T. Y.-C. Kim, L. Gutshall, C. Silverman, S. Khandekar, R. T. Sarisky, and C. C. Kao.** 2002. Mechanism of de novo initiation by the hepatitis C virus RNA-dependent RNA polymerase: role of divalent metals. J. Virol. **76:**12513–12525.
55. **Rieder, E., A. V. Paul, D. W. Kim, J. H. van Boom, and E. Wimmer.** 2000. Genetic and biochemical studies of poliovirus *cis*-acting replication element *cre* in relation to VPg uridylylation. J. Virol. **74:**10371–10380.
56. **Rueckert, R. R.** 1996. Picornaviruses and their replication, p. 507–548. *In* B. Fields (ed.), Virology. Raven Press, New York, N.Y.
57. **Salih, E.** 2005. Phosphoproteomics by mass spectrometry and classical protein chemistry approaches. Mass Spectrometry Rev. **24:**828–846.
58. **Schagger, H., and G. von Jagow.** 1987. Tricine-sodium dodecyl sulfate polyacrylamide gel electrophoresis for the separation of proteins in range from 1 to 100 kDa. Anal. Biochem. **166:**368–379.
59. **Son, H. S., and S. G. Rhee.** 1987. Cascade control of *Escherichia coli* glutamine synthetase. Purification and properties of P_{II} protein and nucleotide sequence of its structural gene. J. Biol. Chem. **262:**8690–8695.
60. **Steitz, T.** 1999. DNA polymerases: structural diversity and common mechanisms. J. Biol. Chem. **274:**17395–17398.
61. **Tellez, A. B., S. Crowder, J. F. Spagnolo, A. A. Thompson, O. B. Peersen, D. L. Brutlag, and K. Kirkegaard.** 2006. Nucleotide channel of RNA-dependent RNA polymerase used for intermolecular uridylylation of protein primer. J. Mol. Biol. **357:**665–675.
62. **Thompson, A. A., and O. Peersen.** 2004. Structural basis for proteolysis-dependent activation of the poliovirus RNA-dependent RNA polymerase. EMBO J. **23:**3462–3471.
63. **Van Dyke, T. A., and J. B. Flanegan.** 1980. Identification of poliovirus polypeptide p63 as a soluble RNA-dependent RNA polymerase. J. Virol. **35:**732–740.
64. **Wedeking, J. E., P. A. Frey, and I. Rayment.** 1996. The structure of nucleotidylated histidine-166 of galactose-1-phosphate uridylyl transferase provides insight into phosphoryl group transfer. Biochemistry **35:**11560–11569.
65. **Xiang, W., A. Cuconati, D. A. Hope, K. Kirkegaard, and E. Wimmer.** 1998. Complete protein linkage map of poliovirus P3 proteins: interaction of polymerase 3D polymerase with VPg and with genetic variants of 3AB. J. Virol. **72:**6732–6741.
66. **Yang, Y., R. Rijnbrand, S. Watowich, and S. M. Lemon.** 2004. Genetic evidence for an interaction between a picornaviral cis-acting RNA replication element and 3CD protein. J. Biol. Chem. **279:**12659–12667.
67. **Yin, J., A. V. Paul, E. Wimmer, and E. Rieder.** 2003. Functional dissection of a poliovirus *cis*-acting replication element [PV-*cre*(2C)]: analysis of single- and dual-*cre* viral genomes and proteins that bind specifically to PV-*cre* RNA. J. Virol. **77:**5152–5166.
68. **Ypma-Wong, M. F., P. G. Dewalt, V. H. Johnson, J. G. Lamb, and B. L. Semler.** 1988. Protein 3CD is the major poliovirus proteinase responsible for cleavage of the P1 capsid precursor. Virology **166:**265–270.
69. **Zhong, W., A. S. Uss, E. Ferrari, J. Y. N. Lau, and Z. Hong.** 2000. De novo initiation of RNA synthesis by hepatitis C virus nonstructural protein 5B polymerase. J. Virol. **74:**2017–2022.